International Journal of Solids and Structures 46 (2009) 4379–4395

Contents lists available at ScienceDirect

International Journal of Solids and Structures

journal homepage: www.elsevier.com/locate/ijsolstr

A 2-D continuous wavelet transform of mode shape data for damage detection of plate structures

Wei Fan, Pizhong Qiao *

Department of Civil and Environmental Engineering, Composite Materials and Engineering Center, Washington State University, Pullman, WA 99164-2910, USA

ARTICLE INFO

Article history:
Received 20 June 2009
Available online 31 August 2009

Keywords:
Damage detection
Continuous wavelet transform
Experimental modal analysis
Mode shapes
Plates and shells
Piezoelectric sensors

ABSTRACT

A two-dimensional (2-D) continuous wavelet transform (CWT)-based damage detection algorithm using "Dergauss2d" wavelet for plate-type structures is presented. The 2-D CWT considered in this study is based on the formulation by Antoine et al. (2004). A concept of isosurface of 2-D wavelet coefficients is proposed, and it is generated to indicate the location and approximate shape or area of the damage. The proposed algorithm is a response-based damage detection technique which only requires the mode shapes of the damaged plates. This algorithm is applied to the numerical vibration mode shapes of a cantilever plate with different types of damage to illustrate its effectiveness and viability. A comparative study with other two 2-D damage detection algorithms, i.e., 2-D gapped smoothing method (GSM) and 2-D strain energy method (SEM), is performed, and it demonstrates that the proposed 2-D CWT-based algorithm is superior in noise immunity and robust with limited sensor data. The algorithm is further implemented in an experimental modal test to detect impact damage in an FRP composite plate using smart piezoelectric actuators and sensors, demonstrating its applicability to the experimental mode shapes. The present 2-D CWT-based algorithm is among a few limited studies in the literature to explore the application of 2-D wavelets in damage detection, and as demonstrated in this study, it can be used as a viable and effective technique for damage identification of plate- or shell-type structures.

1. Introduction

A reliable and effective non-destructive damage detection method is crucial to maintain the safety and integrity of structures. Most non-destructive damage identification methods can be categorized as either local or global damage detection techniques (Doebling et al., 1996). Local damage detection techniques, such as ultrasonic methods and X-ray methods, have their limitations in that the vicinity of damage must be known *a priori* and readily accessible for testing. Hence, the vibration response-based global damage identification method has been developed to overcome these difficulties. The fundamental idea for vibration response-based damage detection is that the damage-induced changes in the physical properties (mass, damping, stiffness, etc.) will cause detectable changes in modal properties (natural frequencies, modal damping, mode shapes, etc.). For instance, reductions in stiffness resulting from the onset of cracks may change the natural frequencies and other modal parameters. Therefore, it is intuitive that damage can be identified by analyzing the changes in vibration features of the structure.

To detect damage using natural frequency shift is the earliest global vibration response method. Salawu presented a comprehensive review (Salawu, 1997) on damage detection methods using the natural frequency shift. Compared to using natural frequencies, the advantages of using mode shapes and their derivatives as a basic feature for damage detection are obvious. First, the mode shapes contain local information, which makes them more sensitive to local damages and enables them to be used directly in multiple damage localization. Second, the mode shapes are less sensitive to environmental effects, such as temperature, than natural frequencies (Farrar and James, 1997). Significant work has been done in localizing damage in beam-type structures using the mode shapes and their derivatives (Hadjileontiadis et al., 2005; Pandey et al., 1991; Ratcliffe, 1997; Stubbs and Kim, 1996; Wang and Qiao, 2008). Many viable damage detection methods for beams have been also successfully extended from one-dimensional (1-D) to two-dimensional (2-D) algorithms for damage detection of plates. Yoon et al. (2005) generalized the 1-D gapped smoothing method (GSM) by Ratcliffe (1997) to 2-D plate-like structural applications. Cornwell et al. (1999) generalized the strain energy-based damage index (DI) method for 1-D beam-type structures by Stubbs and Kim (1996) into 2-D plate-type structures. Hadjileontiadis and Douka (2007) extended the fractal dimension-based crack detection algorithm (Hadjileontiadis et al., 2005) to 2-D for detecting cracks in plate structures.

The application of 1-D wavelet transform to displacement mode shape for damage detection of beam-type structures has been extensively investigated (Liew and Wang, 1998; Quek et al.,

* Corresponding author. Tel.: +1 509 335 5183; fax: +1 509 335 7632.
E-mail address: Qiao@wsu.edu (P. Qiao).

0020-7683/$ - see front matter © 2009 Elsevier Ltd. All rights reserved.
doi:10.1016/j.ijsolstr.2009.08.022

2001; Gentile and Messina, 2003; Douka et al., 2003). Some researchers also extended the application of 1-D wavelet transform to damage detection of plate. Chang and Chen (2004) applied the 1-D wavelet transform on the mode shape data in x- and y-directions separately to detect stiffness loss in plate. Douka et al. (2004) applied a 1-D continuous wavelet analysis on mode shape to localize an all-over part-through crack parallel to one edge of the plate. However, these damage detection techniques are still 1-D in nature since the mode shape data along different directions are treated separately. Recently, the 2-D version of the wavelet transform approach has also become a promising technique for damage detection of plates. Loutridis et al. (2005) applied a 2-D discrete wavelet transform (DWT) of the flexural mode shape to detect cracks in plate. The wavelet coefficients of the detail of the first level decomposition were used to determine the location, length and depth of the crack. Kim et al. (2006) introduced a damage detection technique based on the 2-D multi-resolution analysis of the flexural DI equation by the Haar wavelet. Numerical experiments showed that the wavelet transformation approach could be successfully applied to localize and quantify small damage in the plate using only a few lower mode shapes. Rucka and Wilde (2006) took the 2-D wavelet transform of the fundamental mode shape of plate using the reverse biorthogonal wavelet to locate damage in plate. The wavelet was constructed using the formulation of 2-D discrete wavelet. Both the horizontal and vertical wavelets were taken as tensor products of a 1-D scaling function and a 1-D wavelet function. Then, the transform in two directions were implemented separately. A modulus and angle of the wavelet transform were defined to combine the information of two transforms and adopted as the indicator of damage.

It should be noted that there are two different versions of the wavelet transform, i.e., the continuous wavelet transform (CWT) and the discrete wavelet transform (DWT). The CWT provides precise resolution of wavelet coefficients for damage detection, and it is hence mostly used for feature detection and analysis in signals; whereas the DWT offers a fast algorithm of evaluating wavelet coefficients in discrete resolutions, and it is thus more appropriate for data compression and signal reconstruction (Antoine et al., 2004). Although both the versions have been adopted in aforementioned works, the CWT is more suitable for damage detection problems, due to its excellent performance as a singularity scanner.

The apparent limitation of wavelet transform method is that the rational evaluation of the wavelet transform requires the mode shape measurement with a relatively high spatial resolution. With traditional sensors such as accelerometers, a large number of modal tests are required to achieve such measurement with sufficient spatial resolution and reasonable accuracy. However, with advanced measurement instrument, such as scanning laser vibrometer (SLV) (Qiao et al., 2007a,b), this difficulty can be overcome by its capability of scanning a large number of measurement points synchronously. In addition, the spatial resolution can be further enhanced by the interpolation technique (Rucka and Wilde, 2006).

In this paper, a 2-D CWT-based method is presented for damage detection in plates. In particular, the 2-D CWT of the vibration mode shapes of plate is applied and evaluated to identify the location and shape of damage in the plates. The rest of the paper is organized as follows. The 2-D CWT formulated by Antoine et al. (2004) is briefly introduced in Section 2. The application of the 2-D CWT in damage detection is thoroughly examined using a numerical plate model in Section 3. A comparative study of the present 2-D CWT-based damage detection algorithms with other two established 2-D techniques (i.e., the gapped smoothing method (GSM) and strain energy method (SEM)) is conducted in Section 4. The effectiveness and applicability of the 2-D CWT-based damage detection method is validated in Section 5 via an experimental program using smart piezoelectric sensors.

2. 2-D CWT in damage detection

The 2-D CWT considered in this study is based on the formulation by Antoine et al. (2004). Some of its basic concepts are briefly introduced here. For more information, interested readers are recommended to refer to Antoine et al. (2004).

2.1. 2-D continuous wavelet transform

As in the 1-D case, a 2-D wavelet is an oscillatory, real or complex-valued function $\psi(\vec{x}) \in L^2\left(\mathbb{R}^2, d^2\vec{x}\right)$ satisfying the admissibility condition on real plane $\vec{x} \in \mathbb{R}^2$. $L^2\left(\mathbb{R}^2, d^2\vec{x}\right)$ denotes the Hilbert space of measurable, square integrable 2-D functions. If ψ is regular enough as in most cases, the admissibility condition can be expressed as:

$$\hat{\psi}\left(\vec{0}\right) = 0 \Longleftrightarrow \int_{\mathbb{R}^2} \psi(\vec{x}) d^2\vec{x} = 0 \tag{1}$$

where $\hat{\psi}\left(\vec{k}\right)$ is the Fourier transform of $\psi(\vec{x})$, and $\vec{k} \in \mathbb{R}^2$ is the spatial frequency.

Function $\psi(\vec{x})$ is called a mother wavelet and usually localized in both the position and frequency domains. The mother wavelet ψ can be transformed in the plane to generate a family of wavelet $\psi_{\vec{b},a,\theta}$. A transformed wavelet $\psi_{\vec{b},a,\theta}$ under translation by a vector $\vec{b}$, dilation by a scaling factor a, and rotation by an angel θ can be derived as

$$\psi_{\vec{b},a,\theta}(\vec{x}) = a^{-1}\psi\left(a^{-1}r_{-\theta}\left(\vec{x} - \vec{b}\right)\right) \tag{2}$$

Given a 2-D signal $s(\vec{x}) \in L^2\left(\mathbb{R}^2, d^2\vec{x}\right)$, its 2-D CWT (with respect to the wavelet ψ) $S\left(\vec{b}, a, \theta\right) \equiv T_\psi s$ is the scalar product of s with the transformed wavelet $\psi_{\vec{b},a,\theta}$ and considered as a function of $\left(\vec{b}, a, \theta\right)$ as:

$$\begin{aligned} S\left(\vec{b}, a, \theta\right) &\equiv \left\langle \psi_{\vec{b},a,\theta}, s \right\rangle = a^{-1}\int_{\mathbb{R}^2} \overline{\psi\left(a^{-1}r_{-\theta}\left(\vec{x} - \vec{b}\right)\right)} s(\vec{x}) d^2\vec{x} \\ &= a\int_{\mathbb{R}^2} \overline{\hat{\psi}\left(ar_{-\theta}\left(\vec{k}\right)\right)} e^{i\vec{b}\cdot\vec{k}} \hat{s}\left(\vec{k}\right) d^2\vec{k} \end{aligned} \tag{3}$$

Because Eq. (3) is essentially a convolution of a 2-D signal s with a function $\psi_{\vec{b},a,\theta}$ of zero mean, the transform $S\left(\vec{b}, a, \theta\right)$ is appreciable only in regions of parameter space $\left(\vec{b}, a, \theta\right)$ where $\psi_{\vec{b},a,\theta}$ matches the features of signal s. When ψ is well localized in the spatial frequency domain and position domain, the 2-D CWT acts as a local filter in parameter space.

In the 1-D wavelet analysis, due to its intrinsic characteristic of keeping constant relative bandwidth, the wavelet analysis is more advantageous in detecting singularities at high frequency or small scale than, e.g., the windowed Fourier transform. The same argument applies to the 2-D wavelet analysis. When appropriately designed, the 2-D wavelet transform is also an effective singularity scanner for 2-D signals. As in the 1-D case, the vanishing moments of the wavelet play an important role in detection of singularities. A wavelet ψ usually has vanishing moments $N \geqslant 1$:

$$\int x^\alpha y^\beta \psi(\vec{x}) d^2\vec{x} = 0, \vec{x} = (x, y), \quad 0 \leqslant \alpha + \beta \leqslant N \tag{4}$$

This property improves its efficiency at detecting singularities. A wavelet with vanishing moments N will not see the smooth part of the signal but only detects singularities in the $(N+1)$)th derivatives of the signal.

One typical example of 2-D wavelets is the 2-D Mexican hat wavelet, which is simply the Laplacian of a 2-D Gaussian. Another example is the 2-D Morlet wavelet, which is the product of a plane wave and a Gaussian window. Both the wavelets can find their well-known counterpart in the 1-D wavelet analysis. Their expressions in the position domain are given as follows:

The 2-D Mexican hat wavelet:

$$\psi(\vec{x}) = (2 - |\vec{x}|^2)\exp\left(-\frac{1}{2}|\vec{x}|^2\right) \tag{5}$$

The 2-D Morlet wavelet:

$$\psi(\vec{x}) = \exp\left(i\vec{k_0}\cdot\vec{x}\right)\exp\left(-\frac{1}{2}|\vec{x}|^2\right) + \text{correction term.} \tag{6}$$

2.2. 2-D CWT-based differentiation and filtering

Many researchers have shown that the displacement mode shape itself is not very sensitive to small damage either in beams or plates, even with the high-density mode shape measurement (Khan et al., 1999; Huth et al., 2005). As an effort to enhance the sensitivity of mode shape data to the damage, the derivatives of mode shape are investigated for damage detection (Yoon et al., 2005). In practical damage detection situations, the mode shape derivatives cannot be obtained directly, often requiring the numerical differentiation methods, such as Laplace operator (Cao and Qiao, 2009). An important feature of these numerical differentiation methods is that this process tends to enhance the high frequency noise, therefore requiring a filtering process to compensate for such an effect. Gaussian filtering is one of the most widely used approaches to filter out these high frequency noises. In this case, the desired signal can be obtained by convolving the differentiated mode shape $s(x,y)$ with a Gaussian $g(x,y)$ as:

$$\tilde{s} = g(x,y) * \left(\frac{\partial}{\partial x}\right)^m \left(\frac{\partial}{\partial y}\right)^n s(x,y) \tag{7}$$

where $(*)$ denotes the convolution operator. The 2-D Gaussian is defined as

$$g(x,y) = \exp\left(-\frac{|\vec{x}|^2}{2\sigma^2}\right) = \exp\left(-\frac{x^2+y^2}{2\sigma^2}\right), \quad \vec{x} = (x,y) \tag{8}$$

Using the well-known property of convolution, we obtain

$$\tilde{s} = g(x,y) * \left(\frac{\partial}{\partial x}\right)^m \left(\frac{\partial}{\partial y}\right)^n s(x,y) = \left(\frac{\partial}{\partial x}\right)^m \left(\frac{\partial}{\partial y}\right)^n g(x,y) * s(x,y) \tag{9}$$

If we adopt the derivative of 2-D Gaussian as the mother wavelet and rewrite Eq. (3) as a convolution, we can see

$$S\left(\vec{b},a,\theta\right) = \left(\psi_{a,\theta} * s\right)\left(\vec{b}\right) = \left(\left(\frac{\partial}{\partial x}\right)^m \left(\frac{\partial}{\partial y}\right)^n g_{a,\theta} * s\right)\left(\vec{b}\right) = \tilde{s}_{a,\theta}\left(\vec{b}\right) \tag{10}$$

Hence, the desired differentiated and filtered signal can be obtained by a 2-D wavelet transform of the original mode shape with the derivative of 2-D Gaussian (Dergauss2d) as the wavelet. An example of the derivative of 2-D Gaussian is shown in the position and spatial frequency domains, respectively, in Fig. 1.

2.3. Choice of 2-D wavelet for damage detection in plates

Due to its differentiation and filtering effect, the "Dergauss2d" wavelet becomes an ideal candidate for 2-D CWT-based damage detection in mode shapes of plates. However, which wavelet in the family of Dergauss2d is the most appropriate one for damage detection in plate structures is still a question to be addressed, i.e., the determination of the parameters m, n in the Dergauss2d wavelet $(\partial/\partial x)^m(\partial/\partial y)^n g_{a,\theta}$ is crucial to the success of the algorithm.

One guideline for choosing m and n is that both x and y should be equally weighted to avoid potential false indication of damage area and shape. Therefore, the parameters should be chosen as $m = n$. Another guideline is that the wavelet coefficients of the mode shape from an intact plate should be trivial so that the singularities induced by small damage will be easier to detect. Therefore, the wavelet should have enough vanishing moments (i.e., large enough m and n) so that it is blind to the "healthy" mode shape which appears in the low frequency region. In addition, m and n should also be as small as possible so that it will not significantly magnify the high frequency noises during differentiation.

To determine the appropriate parameters m and n, the Dergauss2d wavelets with different parameters ($m = n = 1,2,3$) are tested on the numerically simulated fundamental mode shape of a healthy rectangular steel plate which is clamped on one side. The results are shown in Fig. 2. It can be seen that for $m = n \geqslant 2$, the Dergauss2d wavelets are blind to the "healthy" mode shape except the singularity at four corners caused by the boundary conditions. Furthermore, the parameters $m = n = 2$ are better than $m = n = 3$ because $m = n = 3$ gives a rougher surface and causes sharper peaks at boundaries due to its higher order differentiation. Therefore, when the first mode shape is used, the Dergauss2d wavelet with $m = n = 2$ is most appropriate for damage detection in plates.

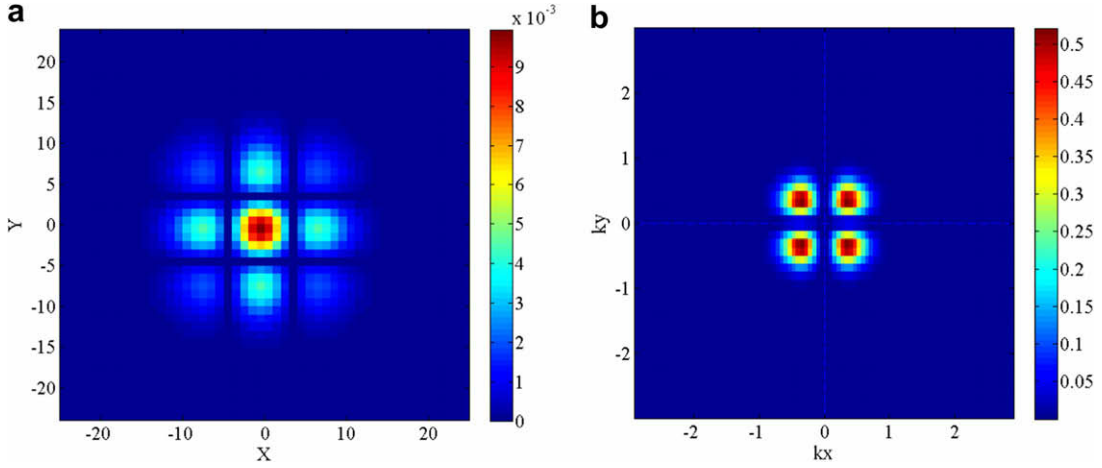

Fig. 1. A Dergauss2d wavelet in (a) position domain and (b) spatial frequency domain $((\partial/\partial x)^m(\partial/\partial y)^n g_{a,\theta}$ with $m = 2$, $n = 2$, $a = 4$, $\theta = 0)$.

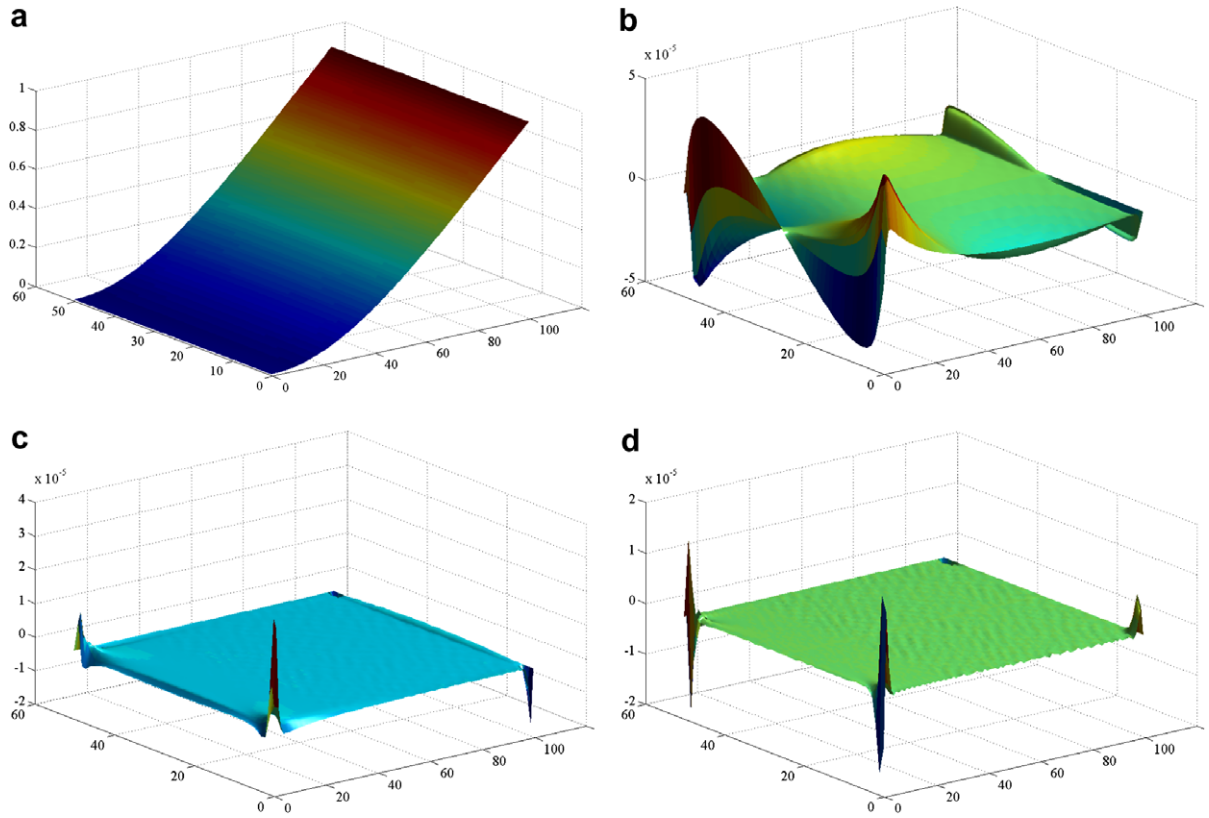

Fig. 2. The 2-D CWT of mode shape of a healthy plate using different Dergauss2d wavelets: (a) mode shape of the healthy plate clamped on one side; (b) wavelet coefficients using Dergauss2d with m, $n = 1$; (c) wavelet coefficients using Dergauss2d with m, $n = 2$; and (d) wavelet coefficients using Dergauss2d with m, $n = 3$.

3. Numerical investigation of damage detection using 2-D CWT

3.1. Description of numerical model

The commercial Finite Element Analysis package ABAQUS is used to conduct an eigenvalue analysis to generate the mode shapes of the damaged plate. For simplicity, the structure is assumed to be a cantilevered steel plate of 1 m width $\times$ 0.125 m depth $\times$ 2 m length with damage. The material is assumed to be steel with Young's modulus $E = 200$ GPa, Poisson's ratio $\nu = 0.2$ and density $\rho = 7850$ kg/m^3. The plate is uniformly divided into approximately 5000 four-node first-order plate elements S4 of size 0.02 m $\times$ 0.02 m and a few three-node first-order plate elements S3. The mode shape data are extracted from all the 101 $\times$ 51 nodes in the model. Three different damage cases are induced in the finite element models: (A) a 0.17 m $\times$ 0.17 m rectangular damaged area centered at $x = 0.52$ m, $y = 0.4$ m with an angle 45° to x-axis; (B) a 0.06 m $\times$ 0.06 m rectangular damaged area centered at $x = 0.45$ m, $y = 0.25$ m; and (C) a 0.1 m length through-thickness crack centered at $x = 0.46$ m, $y = 0.35$ m. For cases (A) and (B), the Young's modulus of the elements in the damaged area is reduced by 30% to simulate the damage-induced stiffness loss. The finite element models with three types of damage scenarios are shown in Fig. 3. The displacement-normalized fundamental mode shapes

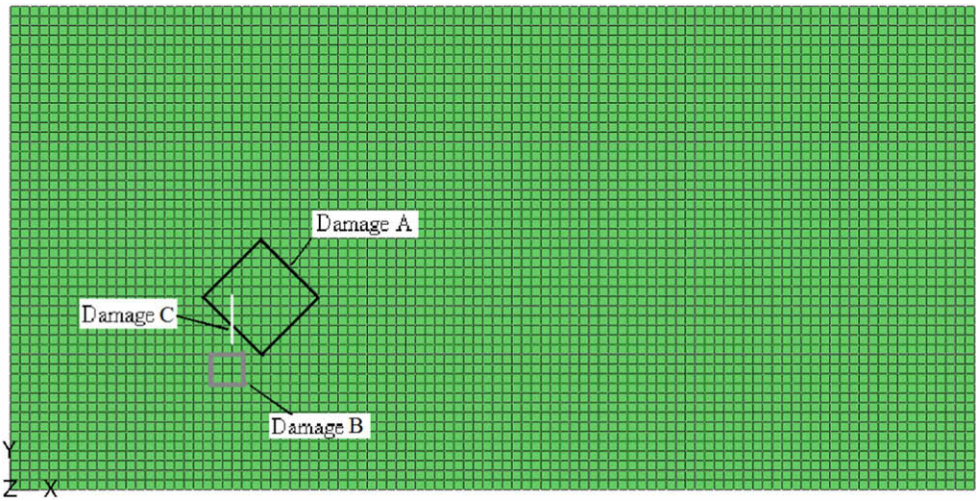

Fig. 3. Finite element model of the plate with three types of damage.

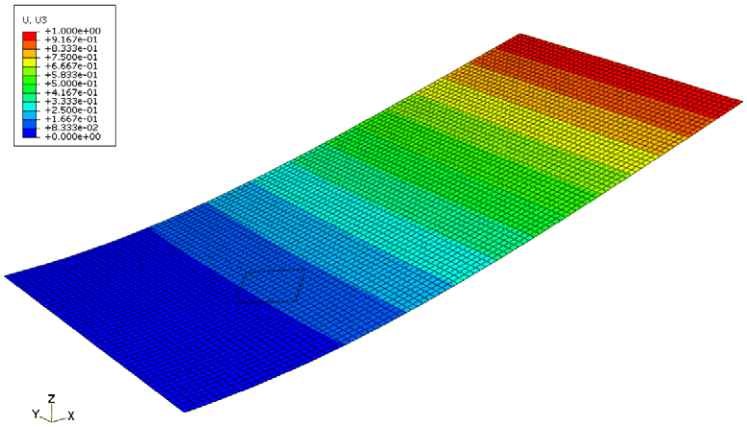

Fig. 4. The fundamental mode shape of the plate with damage A.

of the plate with damage A (i.e., case (A)) are shown in Fig. 4. Comparison between the damaged and healthy plate shows that the displacement mode shape reveals no local features capable of directly indicating the location or shape (area) of the damage.

3.2. Damage detection using the Dergauss2d wavelet

The 2-D CWT is applied to the fundamental mode shape with a Dergauss2d wavelet ($m = n = 2$),

$$S\left(\vec{b},a,\theta\right)=\int_{\mathbb{R}^2} s(\vec{x})\left(\frac{\partial}{\partial x}\right)^2\left(\frac{\partial}{\partial y}\right)^2 g_{a,\theta}\,d^2\vec{x}=\left(\left(\frac{\partial}{\partial x}\right)^2\left(\frac{\partial}{\partial y}\right)^2 g_{a,\theta}*s\right)\left(\vec{b}\right) \tag{11}$$

The fundamental mode shape is treated as a 2-D spatially-distributed signal, in the form of a matrix with 101 rows and 51 columns, corresponding to the displacement at the element nodes along the plate length and width directions, respectively. The spatial resolution of the mode shape is further enhanced by a bivariate

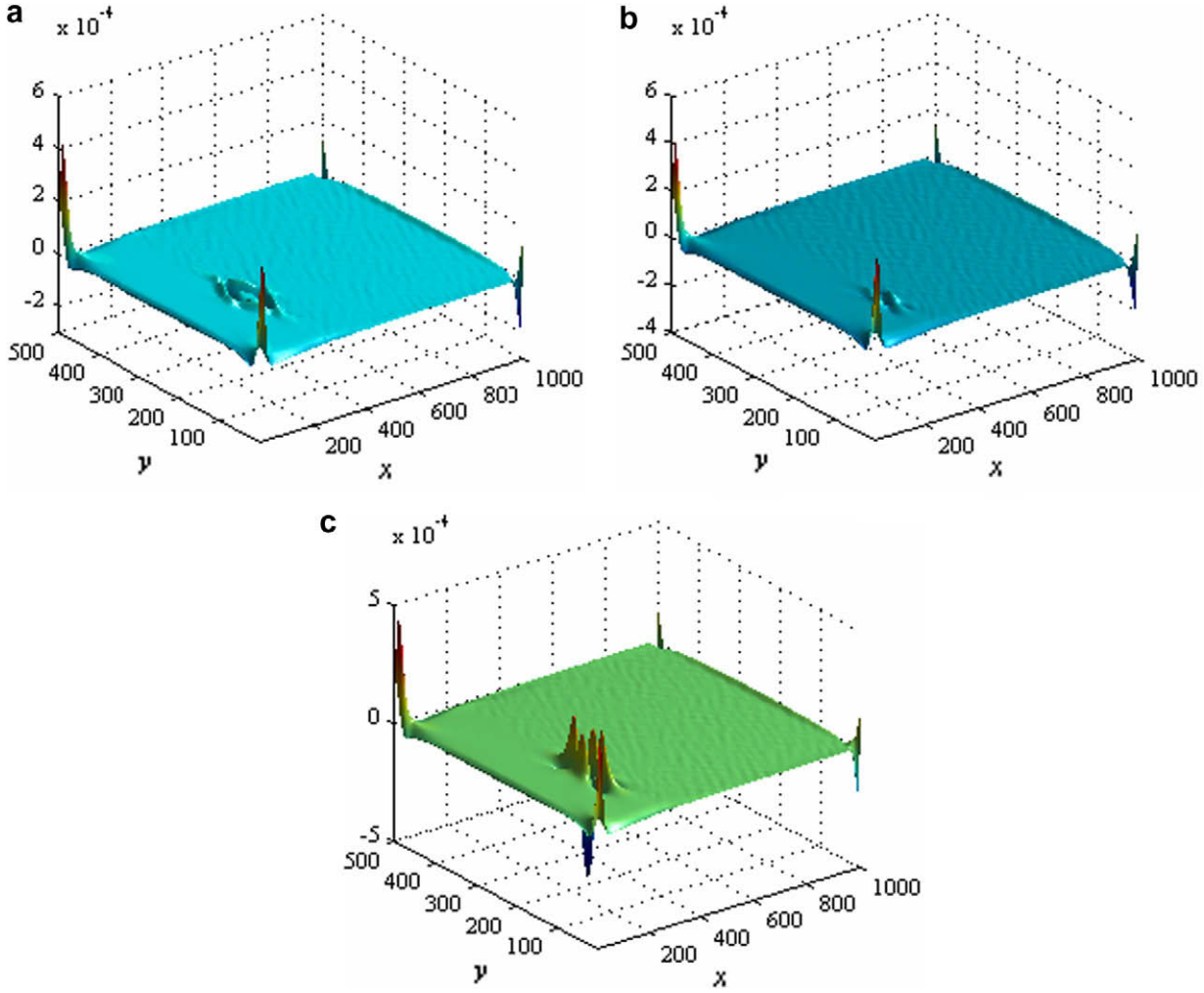

Fig. 5. Wavelet coefficient of fundamental mode shape in three damage cases (with Dergauss2d wavelet, $a = 10$, $\theta = 0$): (a) damage A; (b) damage B; and (c) damage C.

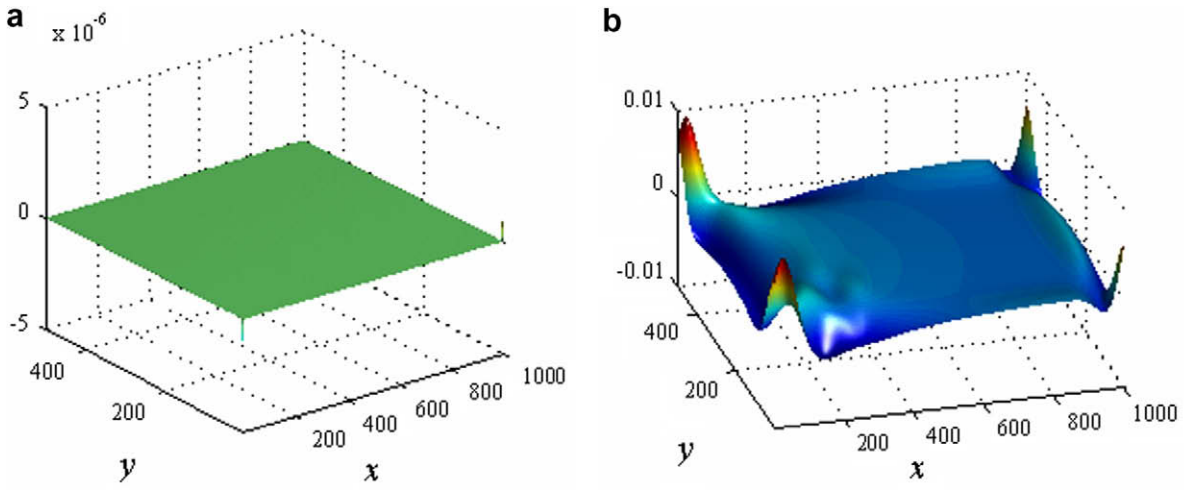

Fig. 6. Wavelet coefficients of the fundamental mode shape in damage B: (a) $a = 1$ and (b) $a = 40$.

cubic spline interpolation. The bivariate cubic spline is constructed as the tensor product of two univariate cubic splines. It can be expressed as the weighted sum of products of two cubic spline functions:

$$f(x,y) = \sum_i \sum_j a(i,j) g_i(x) h_j(y) \tag{12}$$

where $g_i(x)$ and $h_j(y)$ are the cubic spline function in x- and y-directions, respectively. By using the bivariate cubic spline interpolation, the mode shape is oversampled to 1001 rows and 501 columns. The spatial resolution of the data is thus enhanced from 0.02 m to 0.002 m accordingly.

The 2-D CWT is implemented in MATLAB® using the YAW (Yet Another Wavelet) toolbox (Antoine et al., 2004; Jacques et al., 2007) developed by Jacques et al. Once the 2-D CWT is computed, we face a problem of visualization of wavelet coefficients because $S\left(\vec{b}, a, \theta\right)$ is a function of four variables: its position (x,y), scale a, and angle θ. Since the plate in this study is a rectangular oriented in x- and y-directions, the most effective angle θ for our damage detection algorithm should align with x- or y-axis, i.e., $\theta = 0$ or $\pi/2$. Hence, for simplicity, the variable θ is fixed at $\theta = 0$ in this study. The influence of choice of θ will not be our focus in this research. Then, the function $S\left(\vec{b}, a, \theta\right)$ becomes a function $S\left(\vec{b}, a\right)$ of the rest three variables.

If both of the variables a and θ are fixed, the wavelet coefficients obtained from the CWT can also be viewed as a 2-D spatially distributed signal. The wavelet coefficients of the mode shape in the three given damage cases with $a = 10$, $\theta = 0$ are shown in Fig. 5. As shown in Fig. 5, all three types of damage can be correctly detected and located using the chosen variables of $a = 10$, $\theta = 0$. However, the effectiveness of the singularity detection can only be guaranteed by a carefully chosen scale a. When the scale a is not appropriate, the singularity caused by damage can be buried by the numerical errors, measurement noise or boundary distortion. Fig. 6(a) shows the wavelet coefficients in which the singularity induced by damage B is overshadowed by the peaks at corners as $a = 1$. When $a = 40$, the bump in damaged area can barely be noticed as shown in Fig. 6(b). Therefore, simply choosing one single scale a can lead to false indication of damage. A more effective algorithm is thus needed to make full use of the wavelet coefficients with the continuous scale resolution from the 2-D CWT for damage detection and localization.

To develop a viable algorithm, there are two main problems to be addressed. One is to alleviate the distortion of coefficients caused by the boundary condition. Since the CWT is in fact a

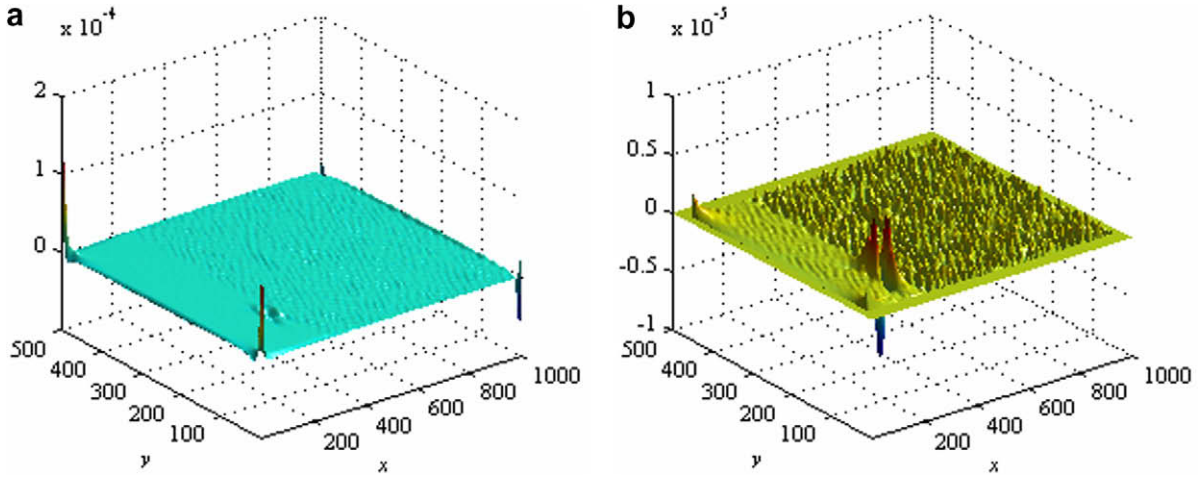

Fig. 7. Wavelet coefficients of the fundamental mode shape in damage B ($a = 6$) before and after boundary distortion treatment: (a) original wavelet coefficients; and (b) wavelet coefficients after the boundary distortion treatment.

convolution of a wavelet and a signal of finite length, the wavelet coefficients will be inevitably distorted by the discontinuity of mode shapes at their ends. The wavelet coefficients could reach an extremely high/low value near the boundaries, although no damage appears in those regions. Those extreme values can even overshadow the singularity caused by damage and make small damage difficult to be detected as shown in Fig. 6(a). This boundary distortion problem has been investigated in the 1-D CWT cases by

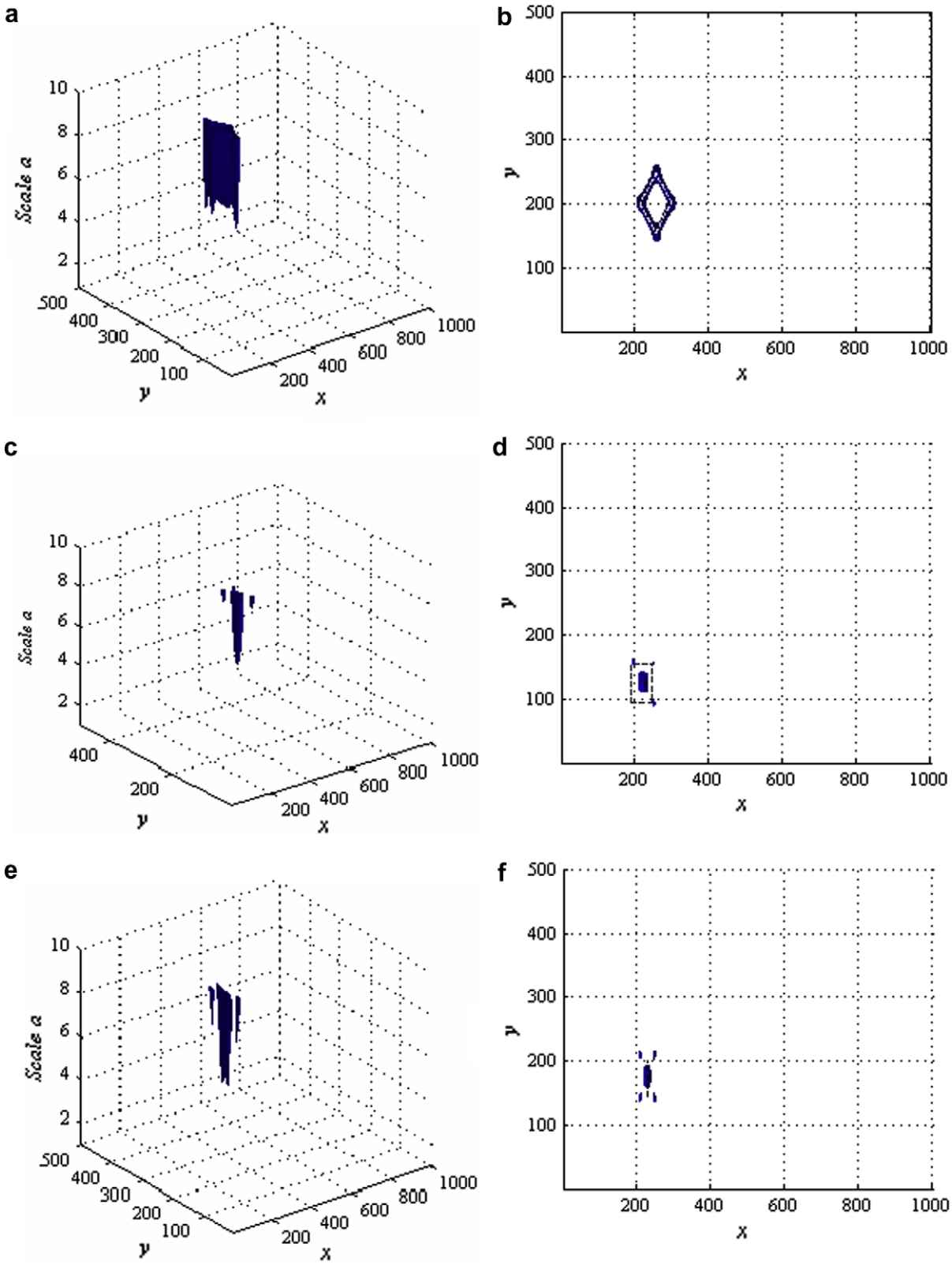

Fig. 8. Isosurfaces generated by the proposed damage detection algorithm (the actual damages are marked in dash lines): (a) 3-D view and (b) top view of isosurface for damage A; (c) 3-D view and (d) top view of isosurface for damage B; (e) 3-D view and (f) top view of isosurface for damage C.

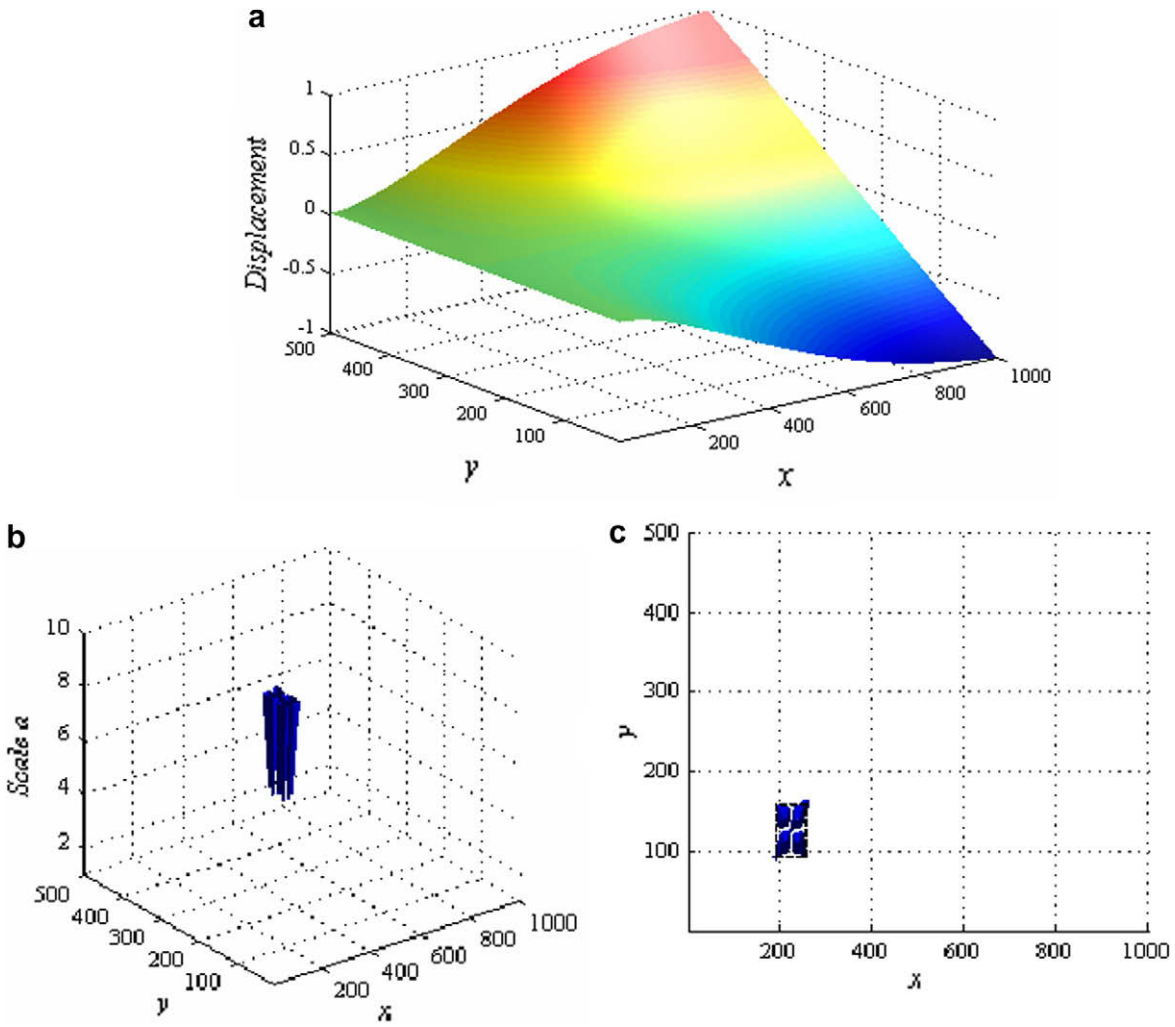

Fig. 9. Isosurface in damage B using the first torsional mode shape: (a) the first torsional mode shape; (b) 3-D view of the isosurface; and (c) top view of the isosurface.

many researchers (Gentile and Messina, 2003; Rucka and Wilde, 2006; Poudel et al., 2007). There are commonly two methods to reduce the boundary effect. One method is to extend the mode shape data beyond its original boundary by the cubic spline extrapolation based on points near the boundaries. It should be noted that the cubic spline extrapolation is merely a way to treat the boundary distortions. Another method is simply to ignore those wavelet coefficients near the boundaries. From the definition of the convolution, it is clear that the boundary distortion can affect the coefficients as far as a half-width of the wavelet away from the boundary. To prevent the extremely distorted value from overshadowing the damage-induced singularity, all the wavelet coefficients in these "boundary effect regions" are cut off or set to zeros. For simplicity, the second method is adopted in this study to treat the boundary distortion problem. The effect of this boundary distortion treatment, i.e., the cut-off of the boundary effect regions, is demonstrated in Fig. 7. As we can see, the elimination of coefficients near boundaries greatly helps the detection of damage in the plate. It should be noted that both the extrapolation method and the "set-to-zero" method will not be capable of detecting the damages close to the boundaries, since both of them smooth out the coefficients information near the boundaries.

Another problem for detecting damage using the wavelet coefficients with the continuous scale resolution is how to visualize a function $S(\vec{b}, a)$ with three independent variables. To solve this problem, an algorithm is proposed to visualize only the singular part of the coefficients instead of visualizing all of the coefficients. The algorithm can be divided into the following four steps:

Table 1
Characteristics of three damage detection algorithms.

Algorithms	Type	Modal parameter requirement	Damage index
2-D CWT	Response-based, only damaged state response required	Mode shape data in damaged beam	Defined at node/ sensor
2-D GSM	Response-based, only damaged state response required	Mode shape data in damaged beam	Defined at node/ sensor
2-D SEM	Model-based	Measured mode shape data in damaged beam and experimental/theoretical/ numerical mode shape data in healthy plate model	Defined at element/ sub-region

Step 1: 2-D CWT. The 2-D CWT of the plate mode shape is computed using MATLAB in continuous scale variation.

Step 2: Boundary distortion treatment. All the wavelet coefficients in the "boundary effect regions" are set to zeros.

Step 3: Threshold value calculation. The maximum and minimum values of the updated wavelet coefficients are calculated. The one with the larger absolute value is multiplied with a threshold ratio between 0 and 1 to generate a threshold value.

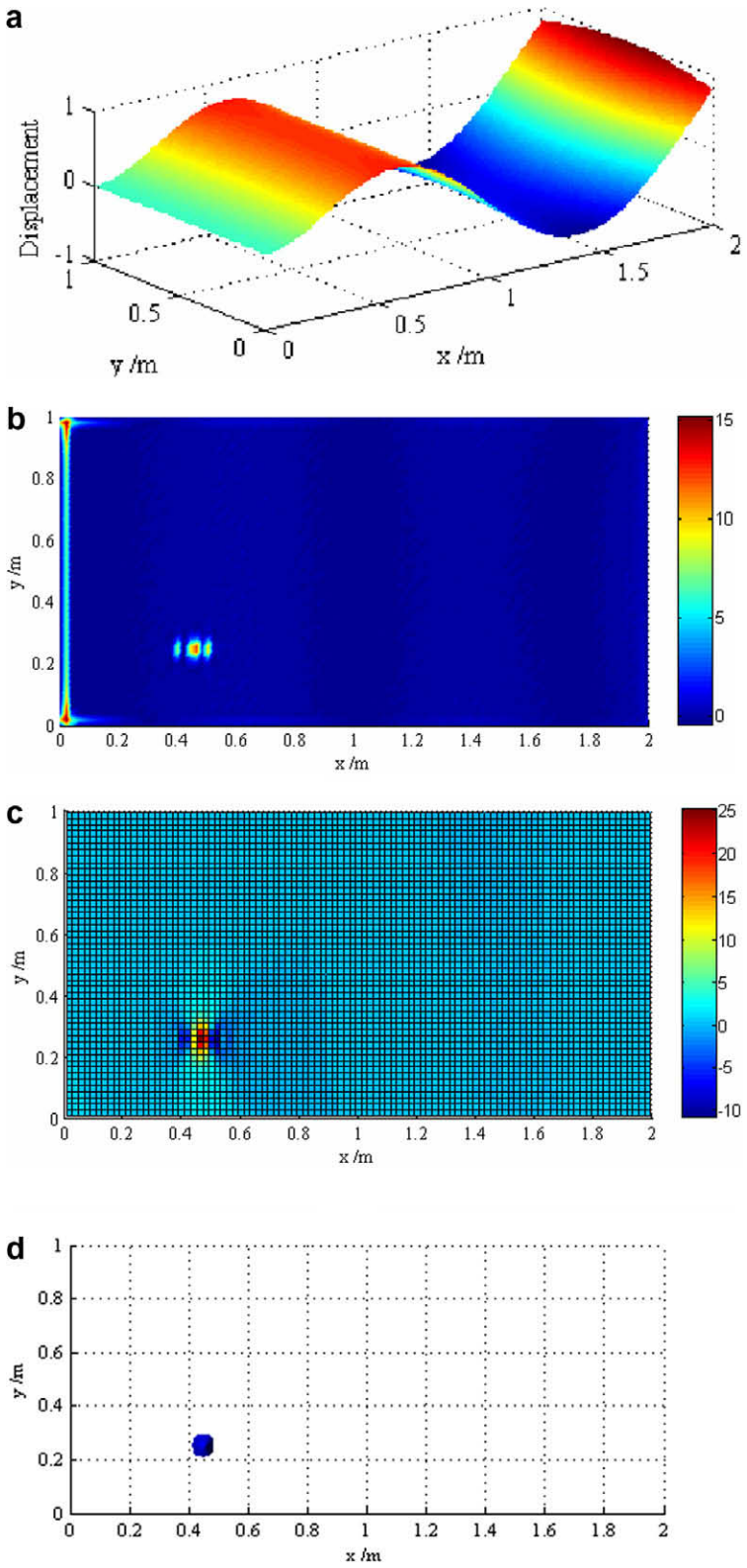

Fig. 10. Damage detection for damage B using the fifth mode shape: (a) the fifth displacement mode shape; (b) normalized damage indices by 2-D GSM; (c) normalized damage indices by 2-D SEM; and (d) isosurface by 2-D CWT.

Step 4: Isosurface generation. The points $\left(\vec{b}, a\right)$ with the threshold value are connected to form an "isosurface" as the way of contour lines connecting points of equal elevation. The isosurface can be directly used to indicate the location and area of the damage.

A MATLAB® code is written to realize this algorithm. For damage detection in all three damage cases, the isosurfaces are generated using this algorithm as shown in Fig. 8. Because the singularity part of the signal lies in the high spatial frequency range, only the wavelet coefficients of low scales are of interest. In this case, the range of the

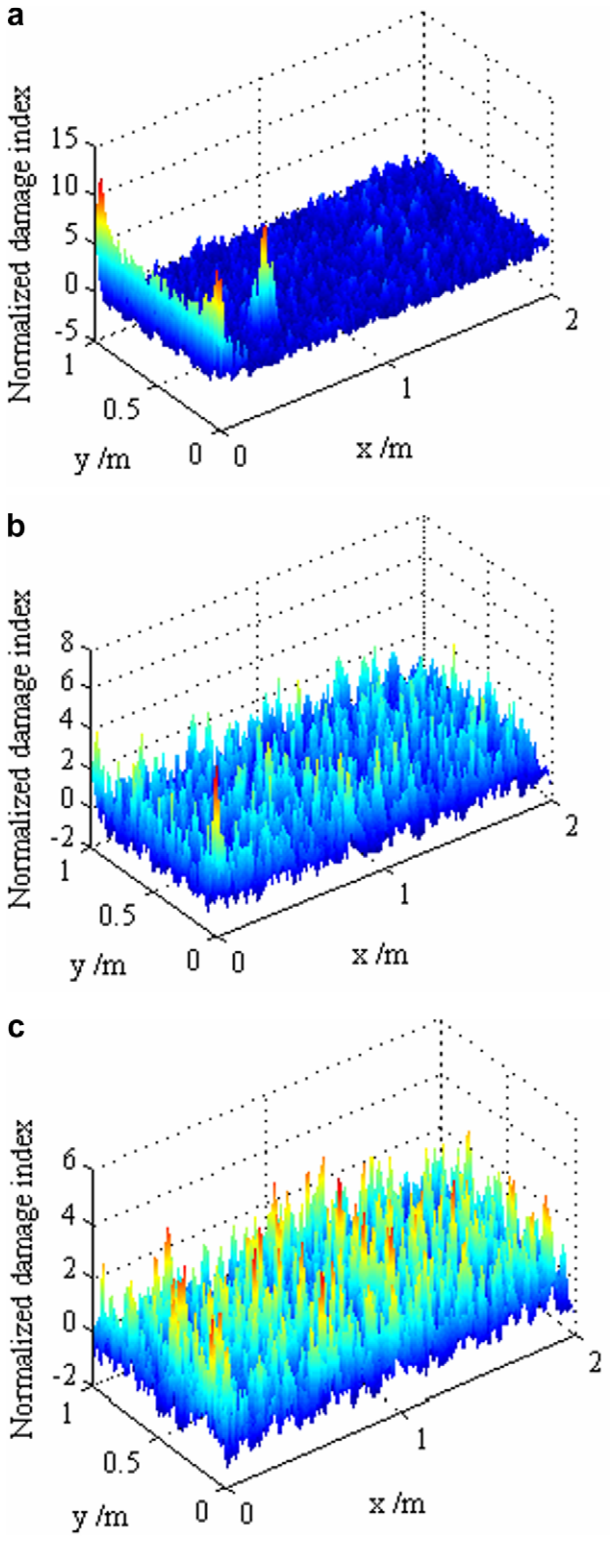

Fig. 11. Normalized damage indices of 2-D GSM using the fifth mode shape data with different noise levels: (a) $\rho = 1 \times 10^{-5}$; (b) $\rho = 5 \times 10^{-5}$; and (c) $\rho = 1 \times 10^{-4}$.

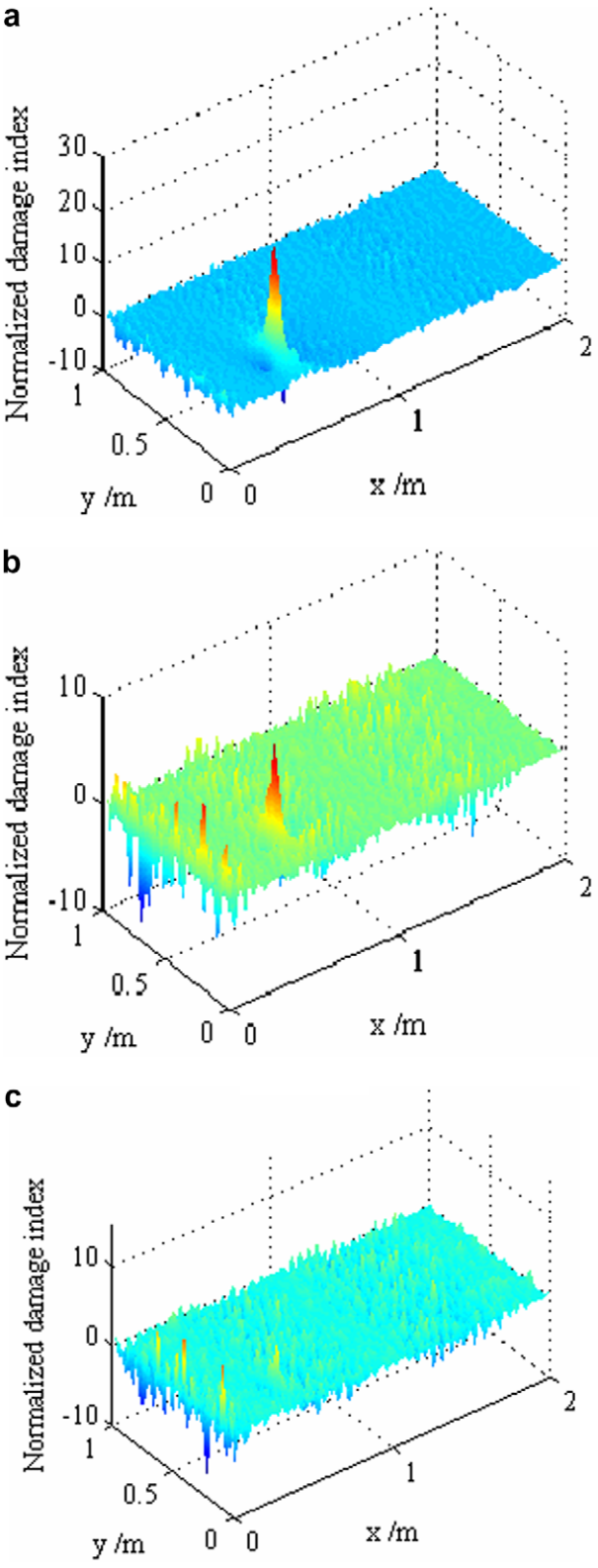

Fig. 12. Normalized damage indices of 2-D SEM using the fifth mode shape data with different noise levels: (a) $\rho = 1 \times 10^{-5}$; (b) $\rho = 5 \times 10^{-5}$; and (c) $\rho = 1 \times 10^{-4}$.

scales in this study is chosen as from $a = 1$ to 10. The threshold ratio t is adjusted to 0.3 based on a few trial analyses to obtain a clear isosurface, although another threshold ratio t in range from 0.1 to 0.4 will also work for the damage detection. It can be seen that in all three damage cases the damage can be correctly located. The isosurface marks the edges of the damaged area, demonstrating that this algorithm is capable of not only locating the damage but also indicating the area and shape of the damage, which is crucial to identify the size and type of the damage.

This algorithm is more advantageous than the one simply using wavelet coefficients from one scale, and the reason is twofold: first, it avoids the false indication of damage caused by an inappropriate choice of a single scale because only the singularities shared by most of the scales can be identified as a damage; second, its noise immunity is more robust because some randomly distributed singular points caused by noise cannot form an clear isosurface. Furthermore, even if an isosurface is formed by noise, a damage-induced isosurface can be easily distinguished from a noise-induced isosurface by its consistency in most of the scales. This feature is further discussed in Section 4.2.

Further investigation shows that this algorithm cannot only be applied on the fundamental bending mode shape but also works on the other mode shapes of the cantilevered plate including the torsional mode shape. Fig. 9 shows the isosurface generated in damage B using the first torsional mode shape. In the torsional mode case, Steps 3 and 4 in the algorithm are slightly adjusted, i.e., the isosurfaces defined by the threshold values from both the maximum and minimum values are overlaid to reflect the complete shape damage; otherwise, only half of the damaged area is shown.

4. Comparative study of damage detection algorithms for plates

To further evaluate performance of the proposed 2-D CWT-based damage detection algorithm, a comparative study of this algorithm with other two established damage detection methods for a plate is conducted. The two other damage detection methods considered are: (1) the two-dimensional gapped smoothing method (2-D GSM) by Yoon et al. (2005), and (2) the two-dimensional strain energy method (2-D SEM) by Cornwell et al. (1999). The comparative study is based on the numerically simulated fifth mode shape of a damaged plate (i.e., damage B in Section 3.2). The choice of this mode is based on its natural frequency change ratio which is a good indicator of the mode sensitivity to the damage event. The nature frequency change ratio in the fifth mode is the largest in the first five modes, and it is hence considered as the most sensitive mode to this specifically given damage (i.e., damage B in this study).

4.1. 2-D GSM and 2-D SEM

The 2-D gapped smoothing method (GSM) adopts the one-dimensional GSM by Ratcliffe (1997) to two-dimensional plate-like

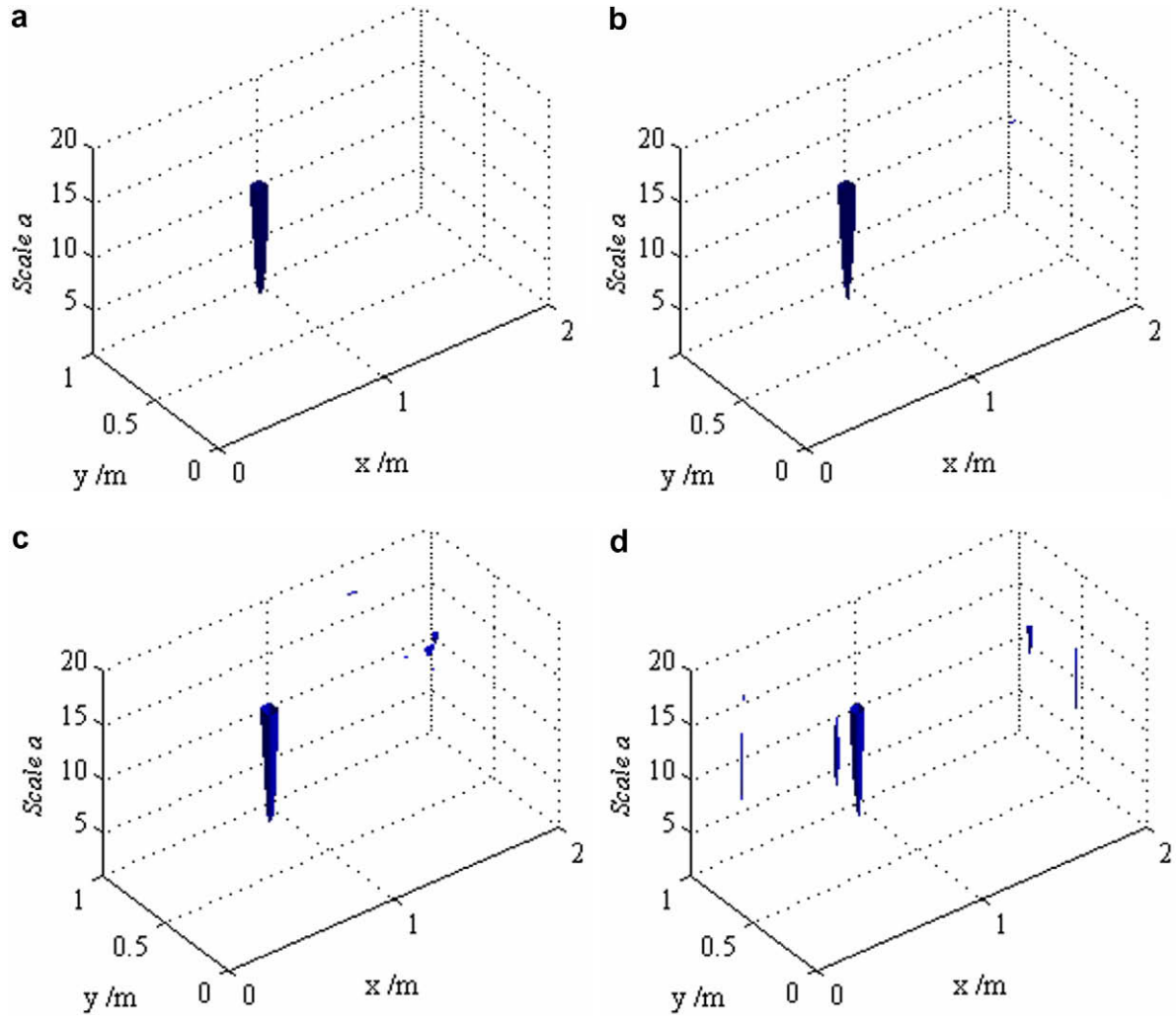

Fig. 13. Isosurfaces of 2-D CWT using the fifth mode shape data with different noise levels: (a) $\rho = 1 \times 10^{-5}$; (b) $\rho = 5 \times 10^{-5}$; (c) $\rho = 1 \times 10^{-4}$; and (d) $\rho = 2.5 \times 10^{-4}$.

structural applications. The curvature mode shape $\nabla^2 w_{ij}$ is first calculated from the displacement mode shape w_{ij} by the central difference approximation at grid point (i,j) as:

$$\nabla^2 w_{ij} = (w_{i+1,j} + w_{i-1,j} - 2w_{i,j}) \Big/ h_x^2 + (w_{i,j+1} + w_{i,j-1} - 2w_{i,j}) \Big/ h_y^2 \quad (13)$$

where h_x and h_y are the horizontal and vertical grid increments, respectively.

Then, a smoothed surface is generated based on the curvature values at its neighboring grid points using the bivariate curve fitting. The smoothed curvature shape is evaluated at grid point (i,j) on the smoothed surface. The damage index β at point (i,j) can be then obtained by

$$\beta_{ij} = \left| \nabla^2 w_{ij} - C_{ij} \right| \quad (14)$$

where C_{ij} is the smoothed curvature at point (i,j).

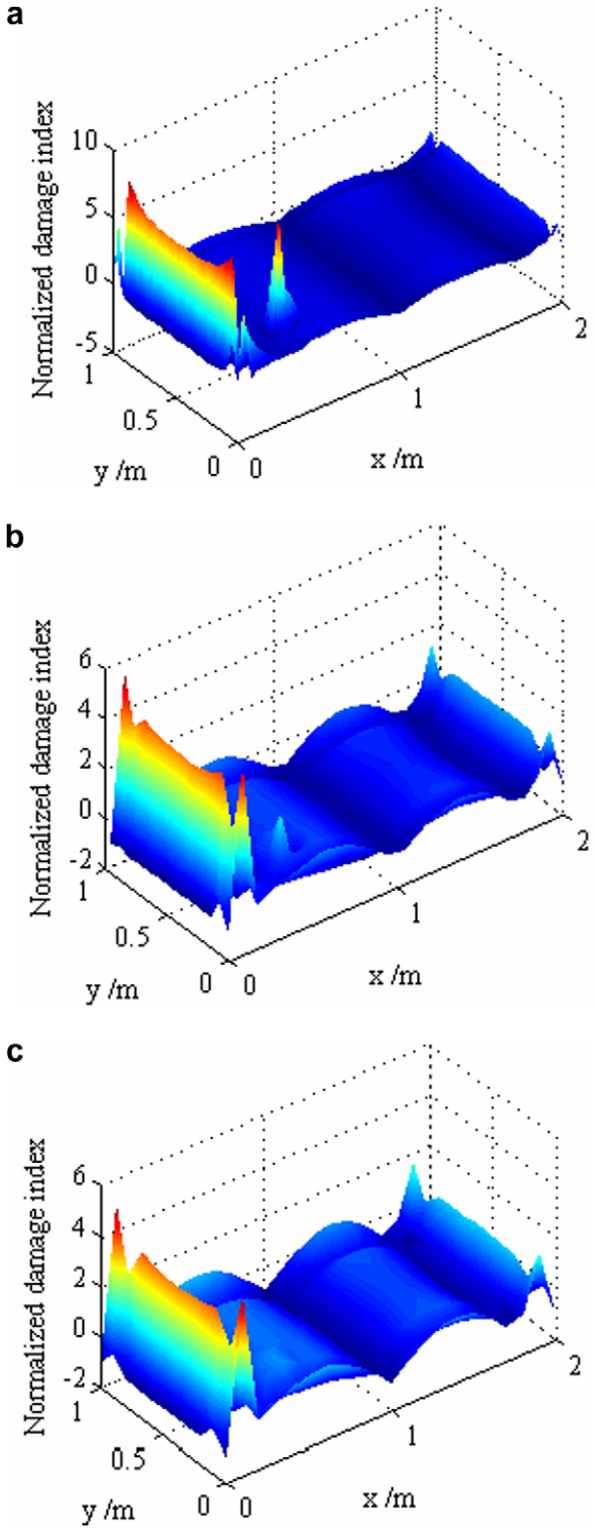

Fig. 14. Normalized damage indices of 2-D GSM using the fifth mode shape data with different sensor spacing: (a) s = 0.04 m; (b) s = 0.08 m; and (c) s = 0.1 m.

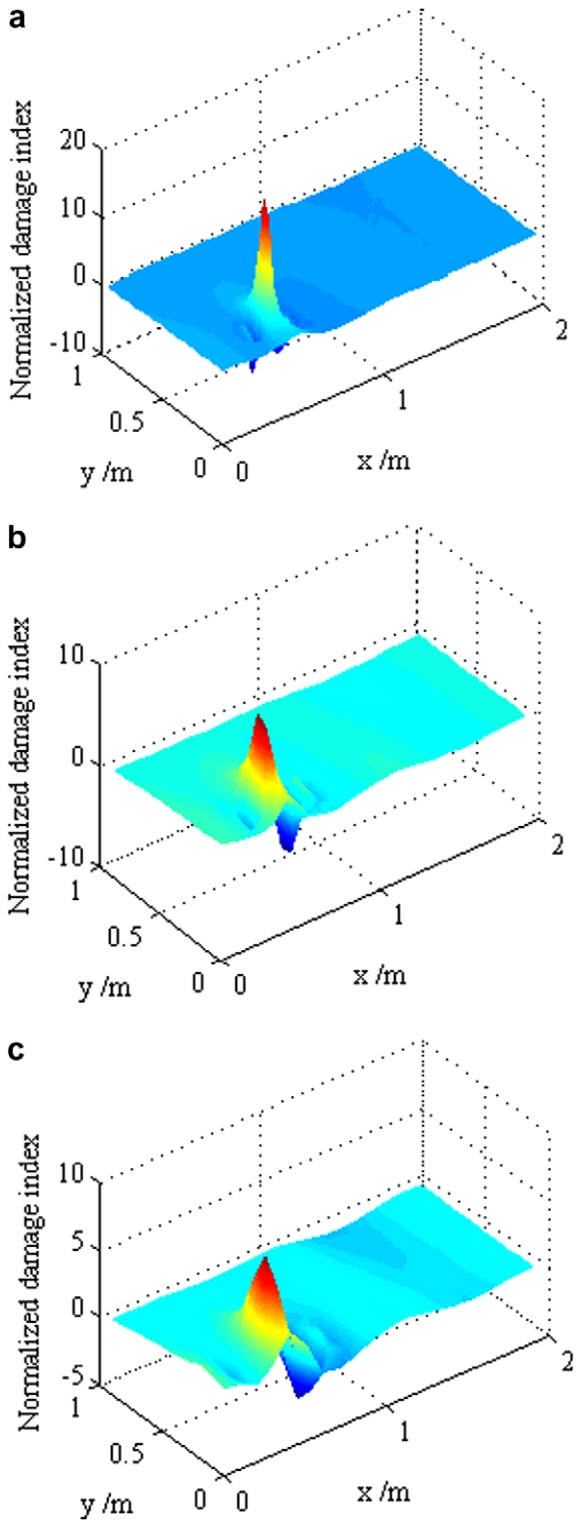

Fig. 15. Normalized damage indices of 2-D SEM using the fifth mode shape data with different sensor spacing: (a) s = 0.04 m; (b) s = 0.08 m; and (c) s = 0.1 m.

While the 2-D strain energy method (SEM) subdivides the plate into N_x subdivisions in the x-direction and N_y subdivisions in the y-direction. It assumes that if the damage is primarily located at a single sub-region, then the fractional strain energy will remain relatively constant in undamaged sub-regions. For plates, the Young's modulus and the Poisson's ratio are assumed to be essentially constant over the whole plate for both the undamaged and damaged modes. The fractional strain energy f_{ijk} in sub-region (i,j) for the kth mode is given by classic plate theory as:

$$f_{ijk}=\frac{\int_{b_j}^{b_{j+1}}\int_{a_i}^{a_{i+1}}\left(\frac{\partial^2 w_i}{\partial x^2}\right)^2+\left(\frac{\partial^2 w_i}{\partial y^2}\right)^2+2\nu\left(\frac{\partial^2 w_i}{\partial x^2}\right)\left(\frac{\partial^2 w_i}{\partial y^2}\right)+2(1-\nu)\left(\frac{\partial^2 w_i}{\partial x\partial y}\right)^2 dxdy}{\int_0^b\int_0^a\left(\frac{\partial^2 w_i}{\partial x^2}\right)^2+\left(\frac{\partial^2 w_i}{\partial y^2}\right)^2+2\nu\left(\frac{\partial^2 w_i}{\partial x^2}\right)\left(\frac{\partial^2 w_i}{\partial y^2}\right)+2(1-\nu)\left(\frac{\partial^2 w_i}{\partial x\partial y}\right)^2 dxdy} \tag{15}$$

where w_k is the kth bending mode shape of the plate; a and b are the dimensions of the plate in x- and y-directions, respectively; the sub-region (i,j) is the rectangular region enclosed by $x=a_i$, $x=a_{i+1}$, $y=b_j$ and $y=b_{j+1}$.

The damage index β at sub-region (i,j) can be obtained by

$$\beta_{ij}=\frac{\sum_{k=1}^{m} f_{ijk}^{*}}{\sum_{k=1}^{m} f_{ijk}} \tag{16}$$

where f_{ijk} and f_{ijk}^{*} are the fractional strain energy from the healthy and damaged plate, respectively.

For the sake of comparison, both the damage index in the 2-D GSM and 2-D SEM are normalized. A normalized damage index Z at point (for the 2-D GSM) or sub-region (i,j) (for the 2-D SEM) can be obtained using

$$Z_{ij}=\frac{\beta_{ij}-\overline{\beta}}{\sigma_\beta} \tag{17}$$

where $\overline{\beta}$ and σ_β represent the mean and standard deviation of the damage indices, respectively. Usually, a damage detection criterion can be set when the normalized damage index Z_{ij} is larger than 2. The main characteristics of three damage detection algorithms are summarized in Table 1.

The 2-D GSM and 2-D SEM are directly applied to the numerical finite element mode shape of the damaged plate to verify their ability to detect the damage. The normalized damage indices are shown in Fig. 10. The results show that both the methods are able to detect the location of damage B in the ideal situation. Like the 2-D CWT, the 2-D GSM also works in sizing the damage area, although without special treatment, a similar boundary distortion problem occurs at the clamped end of the plate.

4.2. Effect of measurement noise

In experimental modal testing, measurement noises are inevitable. To evaluate the robustness of a damage detection method, it is essential to investigate its noise immunity performance. In order to simulate the effect of measurement noise, a series of normally distributed random numbers are added to the numerical mode shapes to generate the noise-contaminated mode shapes. The original numerical mode shape data are extracted from all the 101×51 nodes in the finite element model. The new mode shape data can be expressed as:

$$w'(x,y)=w(x,y)+\rho\cdot r\cdot w_{\mathrm{rms}} \tag{18}$$

where w' and w are the displacement mode shapes with and without noise, respectively; r is the normally distributed random variables with a mean equal to zero and a variance equal to 1; ρ is the random noise level; and w_{rms} is the root-mean-square of the displacement mode shape.

Based on the noisy mode shape data established by Eq. (18), the effect of measurement noise at different levels is illustrated in Figs. 11–13. As shown in Fig. 11, the 2-D GSM can only correctly detect the damage when $\rho=1\times10^{-5}$, with a large boundary distortion at the clamped end. After the noise level reaches $\rho=5\times10^{-5}$, the 2-D GSM cannot detect the damage anymore. Fig. 12 indicates that the 2-D SEM offers a better noise immunity than the 2-D GSM. The

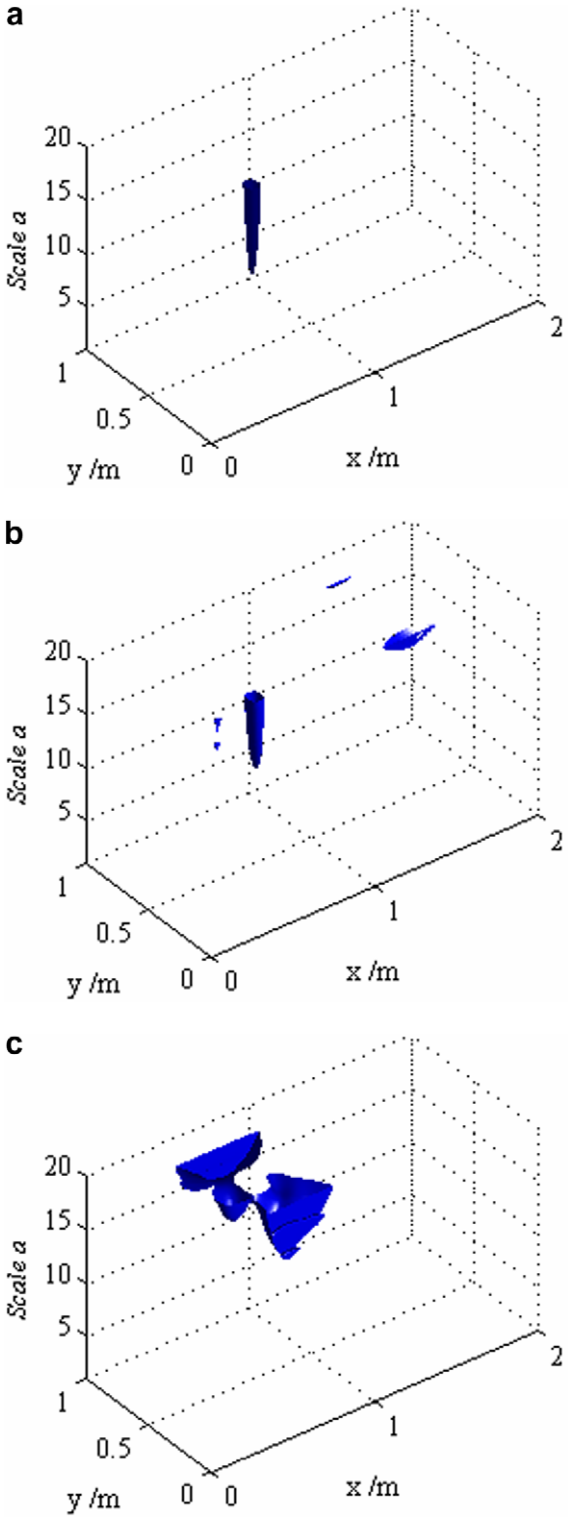

Fig. 16. Isosurfaces of 2-D CWT using the fifth mode shape data with different sensor spacing: (a) $s=0.04$ m; (b) $s=0.08$ m; and (c) $s=0.1$ m.

damage can be correctly localized when $\rho = 5 \times 10^{-5}$, if the boundary distortion is neglected. But in the case of $\rho = 1 \times 10^{-4}$, the damage can barely be noticed. Compared to both the 2-D GSM and 2-D SEM, the 2-D CWT clearly exhibits its superior noise immunity. As shown in Fig. 13, the damage location can be successfully identified when $\rho = 1 \times 10^{-4}$. Further investigation shows that the 2-D CWT is effective in detecting the given damage with noise level as high as $\rho = 2.5 \times 10^{-4}$. Although in the case of $\rho = 2.5 \times 10^{-4}$, some pieces of isosurface caused by noise begin to appear, it is not difficult to distinguish these isosurfaces from the one caused by real damage by its pattern. Since these isosurfaces are caused by random noise, their existences and shapes are not as consistent from the low scale to high scale as the real one.

4.3. Effect of sensor spacing

In experimental modal analysis, the mode shapes can be only measured at a relatively small number of locations, especially for *in situ* experiments. The sparse distribution of sensors will often pose difficulties for damage detection algorithms to effectively detect and localize the damage. Even though the novel measurement systems, such as scanning laser vibrometer (SLV), can be adopted to obtain high-density mode shape data in laboratory-scale experiments, the robustness of the damage detection algorithms under the limited measured data points is still of interest for their practicality for *in situ* experiment. In order to evaluate the effect of different sensor spacing, the mode shape data are extracted from in the finite element model with three different intervals ($s = 0.04$ m, 0.08 m and 0.10 m) for the numerically simulated plate with in-plane dimensions of 1 m $\times$ 2 m. In these three cases, the extracted mode shape data form a matrix of 51×26, 26×13, and 21×11, respectively, for $s = 0.04$ m, 0.08 m, and 0.10 m.

Figs. 14–16 illustrate the effect of different sensor spacing. As shown in Fig. 14, the 2-D GSM can only correctly detect the damage when $s = 0.08$ m if the large boundary distortion at the clamped end is neglected. But the damage-induced singularity can barely be noticed after the noise level reaches $s = 0.10$ m. In Fig. 15, the 2-D SEM can correctly indicate the damage in all three sensor spacing cases. However, its ability to localize the damage gradually decreases when the sensor spacing increases. As shown in Fig. 16, the 2-D CWT shows its ability to detect and localize the damage before the sensor spacing reaches $s = 0.08$ m. But it fails to detect the damage when $s = 0.10$ m, similar to the case of the 2-D GSM. The results show that the robustness of the 2-D CWT damage detection algorithms under the limited measured data points is as good as the 2-D GSM, but not as good as the 2-D SEM. However, it should be noted that both the 2-D GSM and 2-D CWT are the response-based algorithms; while the 2-D SEM is a model-based algorithm, requiring a relatively accurate numerical/analytical model of the healthy structure, which is not feasible for almost all the *in situ* structural tests.

5. Experimental verification

5.1. Experimental set-up and modal analysis

To demonstrate the 2-D CWT-based damage detection algorithm, a 0.508 $\times$ 0.254 $\times$ 0.00318 m (20 $\times$ 10 $\times$ 0.125 in.) FRP composite plate is experimentally tested. The plate is clamped at one end by a steel anchor beam. An artificially-induced impact damage with an approximate diameter of 20.3 mm (0.8 in.) is induced in the plate before the modal testing.

The modal testing of the damaged plate is conducted with a roving excitation test. The plate is uniformly divided into 20 $\times$ 10 elements by the grid lines as shown in Fig. 17. The plate is subjected to a dynamic pulse load applied at each grid point using modally tuned hammer (PCB 652B10). A total of 20 $\times$ 9 grid points are tested corresponding to an actual spatial sampling distance of 25.4 mm (1.0 in.). The response measurements are made using one accelerometer (PCB 352C68) to record the response of the structure. The analog signals then pass a low-pass anti-aliasing filter to prevent the aliasing problem. A Krohn–Hite 3382 eight-pole dual channel filter is employed to filter out the high frequency signals above the cut-off frequency of 250 Hz. The filtered signals are then digitized and collected by the data acquisition system dSPACE CP1103 at the sampling frequency of 500 Hz. The measurements at

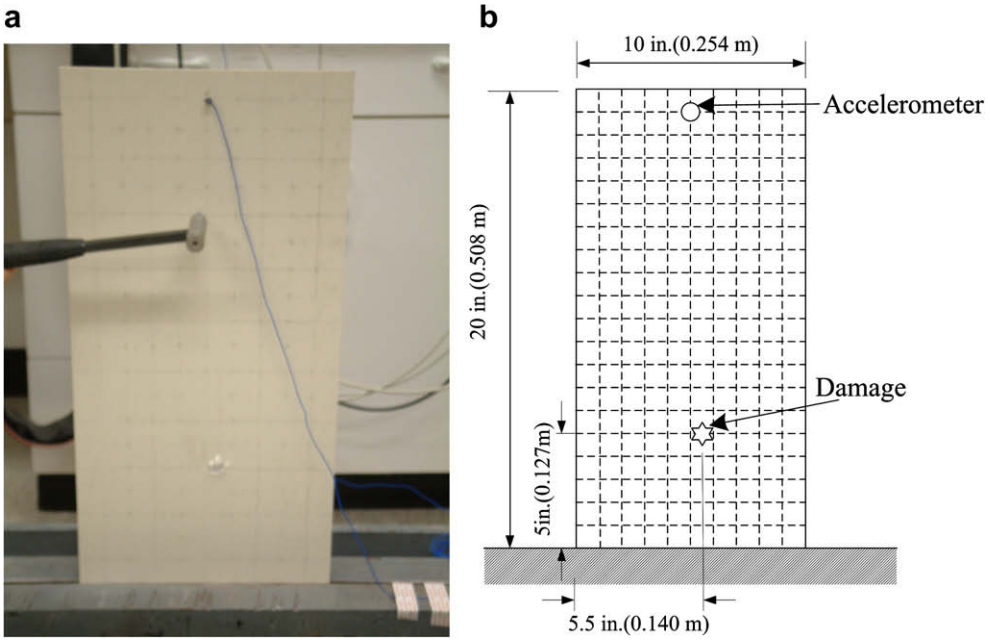

Fig. 17. A cantilevered FRP composite plate with artificially-induced impact damage for modal testing: (a) test specimen and (b) grid for response measurement using accelerometer.

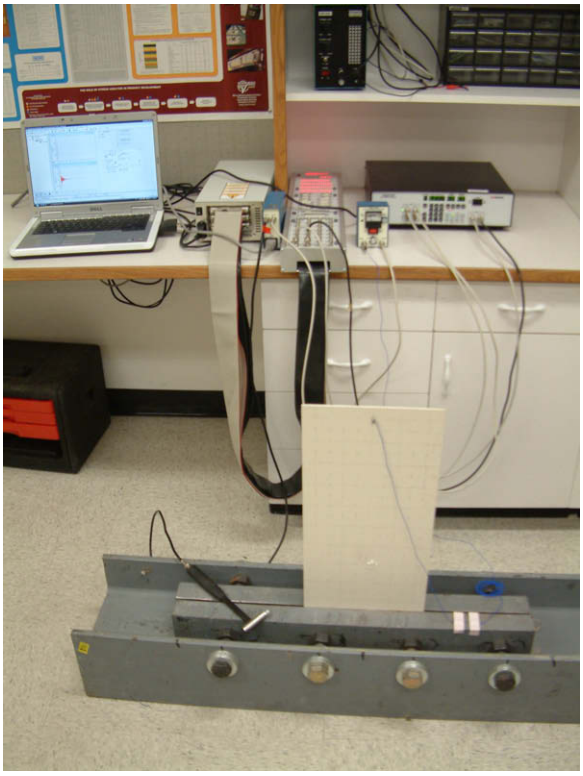

Fig. 18. Experimental set-up and data acquisition system for modal analysis.

each point are repeated 16 times, and the synchronized time histories from the excitation and response measurements are averaged to enhance the signal-to-noise ratio (SNR). The complete experimental set-up is shown in Fig. 18. Then, the frequency–response functions (FRFs) of these tested points are calculated from these excitation and response time-histories. A typical FRF curve and its coherence curve from the test are illustrated in Fig. 19. Then, these FRF curves are imported to the modal analysis program ME-Scope for curve fitting and modal extraction. Fig. 20 shows the fifth mode shape of the composite plate, which is used for the damage detection in the next section.

5.2. Damage detection results using 2-D CWT-based algorithm

The proposed 2-D CWT-based algorithm is applied to the experimentally obtained fifth mode shape of the composite plate (see Fig. 20) for damage detection. First, the mode shape data are oversampled by 10 using the bivariate cubic spline interpolation to enhance the spatial sampling distance from 25.4 mm (1.0 in.) to 2.54 mm (0.10 in.). Then, the 2-D CWT-based damage detection algorithm is applied to the oversampled data. The investigation shows that in this case a scale from 1 to 10 is sufficient for damage detection. The threshold value is set to 0.4 in this case, although any threshold value between 0.3 and 0.5 can give a relatively clear isosurface indicating the damage. The results from the algorithm are shown in Fig. 21. The isosurface in Fig. 21 accurately indicate the location of the damage and illustrate the approximate shape of the damage. Although there is a small piece of noise-induced isosurface in Fig. 21, it can be easily distinguished from the "real" damage-induced isosurface by its pattern as mentioned in Section 4.2. In conclusion, the results of this experiment demonstrate the validity and effectiveness of the 2-D CWT-based damage detection algorithm being applied to the experimental mode shape data.

6. Conclusions

A 2-D CWT-based damage detection algorithm using "Dergauss2d" wavelet for plate-type structures is presented. An isosurface of 2-D wavelet coefficients is generated to indicate the location and approximate shape (or area) of the damage. The viability of this method is demonstrated by analyzing the numerical and experimental mode shapes of a cantilevered plate. The proposed algorithm is a response-based damage detection technique

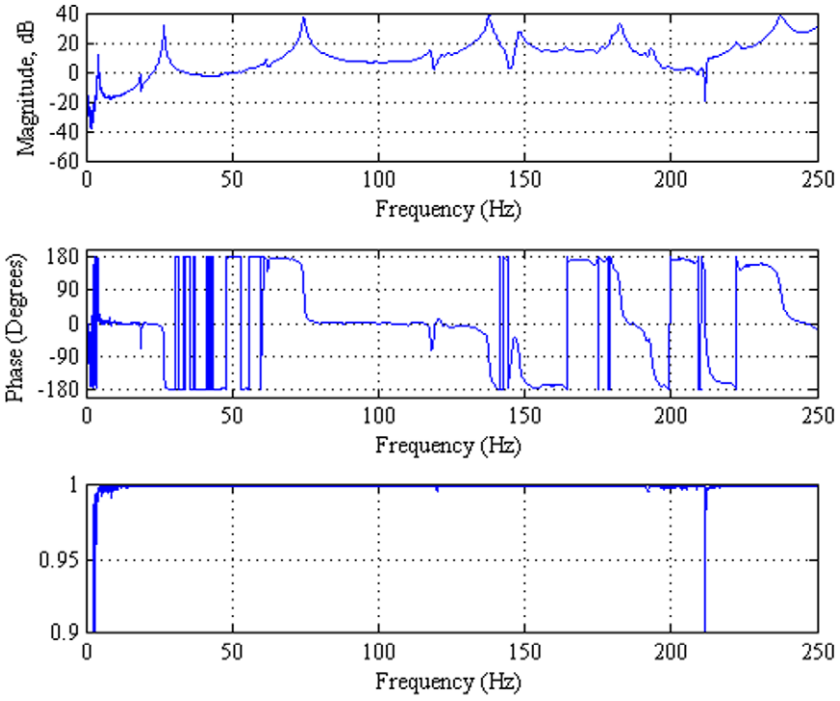

Fig. 19. FRF and coherence curves for acceleration measurement at a typical point.

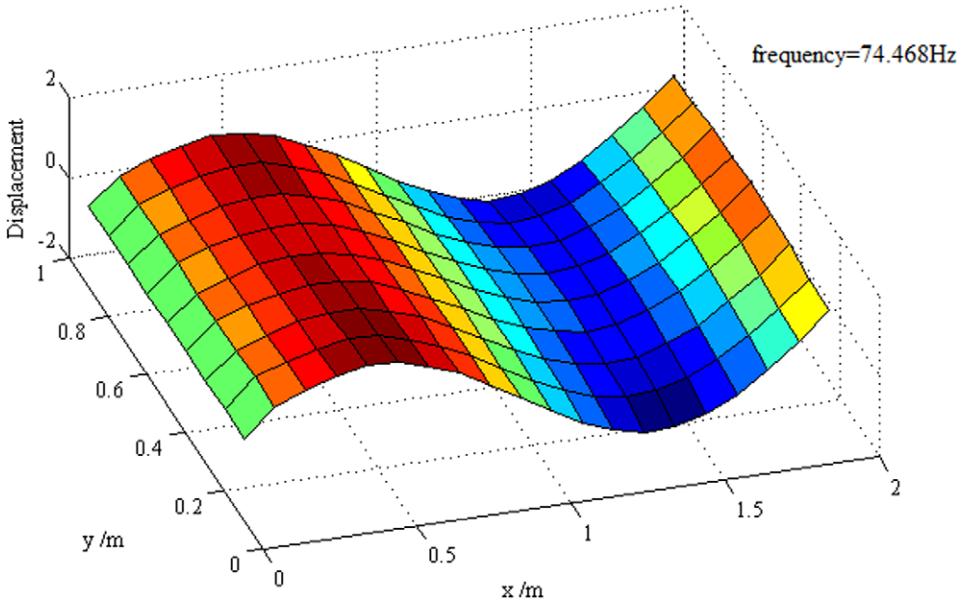

Fig. 20. The fifth mode shape of the composite plate from the experimental modal analysis.

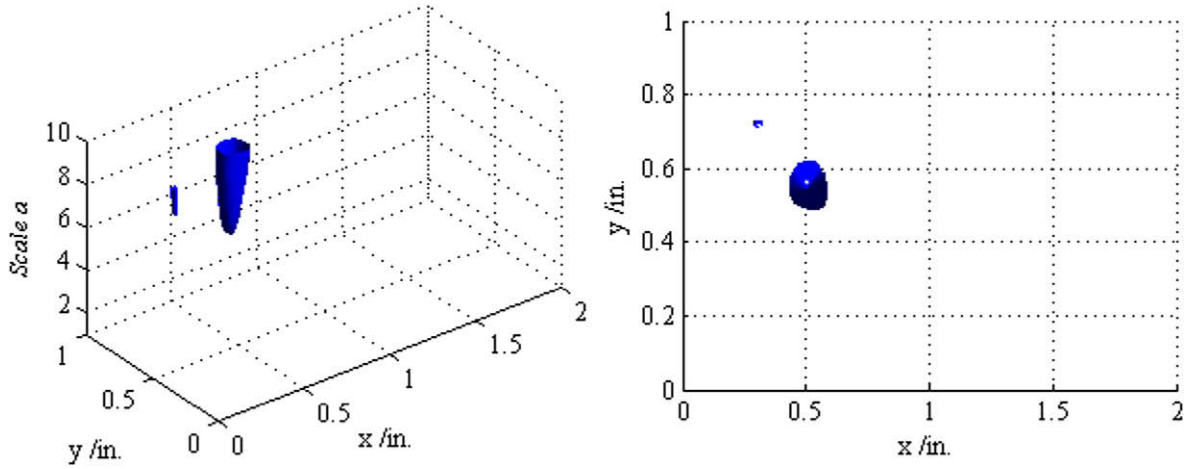

Fig. 21. Isosurface of 2-D CWT using the fifth mode shape data from experimental modal analysis: (a) 3-D view and (b) top view.

which only requires the mode shapes of the plate after damage. A comparative study with two other 2-D damage detection algorithms, i.e., 2-D GSM and 2-D SEM, shows that the proposed 2-D CWT-based algorithm is superior in noise immunity and robust under limited sensor data. Therefore, the proposed algorithm is more advantageous in laboratory or *in situ* damage detection experiment.

This study paves some foundation for the application of 2-D CWT-based damage detection algorithm for plate- or shell-type structures. However, more experiments are needed to demonstrate the practicality of this method for *in situ* damage detection. Studies towards the application of statistical pattern recognition techniques for identification of damage severity and types should be the subject of future research.

Acknowledgments

This study is partially supported by the Alaska University Transportation Center (AUTC) (Contract/Grant No. DTRT06-G-0011) on Smart FRP Composite Sandwich Bridge Decks in Cold Regions.

References

Antoine, J.P., Murenzi, R., Vandergheynst, P., et al., 2004. Two-Dimensional Wavelets and Their Relatives. Cambridge University Press, Cambridge.

Cao, M.S., Qiao, P.Z., 2009. Novel Laplacian scheme and multi-resolution modal curvatures for structural damage identification. Mechanical Systems and Signal Processing 23 (4), 1223–1242.

Chang, C.C., Chen, L.W., 2004. Damage detection of a rectangular plate by spatial wavelet based approach. Applied Acoustics 65 (8), 819–832.

Cornwell, P., Doebling, S.W., Farrar, C.R., 1999. Application of the strain energy damage detection method to platelike structures. Journal of Sound and Vibration 224 (2), 359–374.

Doebling, S.W., Farrar, C.R., Prime, M.B. et al., 1996. Damage Identification and Health Monitoring of Structural and Mechanical Systems from Changes in their Vibration Characteristics: A Literature Review. Los Alamos National Laboratory Report (LA-13070-MS).

Douka, E., Loutridis, S., Trochidis, A., 2003. Crack identification in beams using wavelet analysis. International Journal of Solids and Structures 40 (13–14), 3557–3569.

Douka, E., Loutridis, S., Trochidis, A., 2004. Crack identification in plates using wavelet analysis. Journal of Sound and Vibration 270 (1–2), 279–295.

Farrar, C.R., James, G.H., 1997. System identification from ambient vibration measurements on a bridge. Journal of Sound and Vibration 205 (1), 1–18.

Gentile, A., Messina, A., 2003. On the continuous wavelet transforms applied to discrete vibrational data for detecting open cracks in damaged beams. International Journal of Solids and Structures 40 (2), 295–315.

Hadjileontiadis, L.J., Douka, E., 2007. Crack detection in plates using fractal dimension. Engineering Structures 29 (7), 1612–1625.
Hadjileontiadis, L.J., Douka, E., Trochidis, A., 2005. Fractal dimension analysis for crack identification in beam structures. Mechanical Systems and Signal Processing 19 (3), 659–674.
Huth, O., Feltrin, G., Maeck, J., et al., 2005. Damage identification using modal data: Experiences on a prestressed concrete bridge. Journal of Structural Engineering-ASCE 131 (12), 1898–1910.
Jacques, L., Coron, A., Vandergheynst, P. et al., 2007. Yet Another Wavelet Toolbox. Available from: <http://rhea.tele.ucl.ac.be/yawtb/>.
Khan, A.Z., Stanbridge, A.B., Ewins, D.J., 1999. Detecting damage in vibrating structures with a scanning LDV. Optics and Lasers in Engineering 32 (6), 583–592.
Kim, B.H., Kim, H., Park, T., 2006. Nondestructive damage evaluation of plates using the multi-resolution analysis of two-dimensional Haar wavelet. Journal of Sound and Vibration 292 (1–2), 82–104.
Liew, K.M., Wang, Q., 1998. Application of wavelet theory for crack identification in structures. Journal of Engineering Mechanics-ASCE 124 (2), 152–157.
Loutridis, S., Douka, E., Hadjileontiadis, L.J., et al., 2005. A two-dimensional wavelet transform for detection of cracks in plates. Engineering Structures 27 (9), 1327–1338.
Pandey, A.K., Biswas, M., Samman, M.M., 1991. Damage detection from changes in curvature mode shapes. Journal of Sound and Vibration 145 (2), 321–332.
Poudel, U.P., Fu, G.K., Ye, H., 2007. Wavelet transformation of mode shape difference function for structural damage location identification. Earthquake Engineering & Structural Dynamics 36 (8), 1089–1107.
Qiao, P.H., Lu, K., Lestari, W., et al., 2007a. Curvature mode shape-based damage detection in composite laminated plates. Composite Structures 80 (3), 409–428.
Qiao, P.Z., Lestari, W., Shah, M.G., et al., 2007b. Dynamics-based damage detection of composite laminated beams using contact and noncontact measurement systems. Journal of Composite Materials 41 (10), 1217–1252.
Quek, S.T., Wang, Q., Zhang, L., et al., 2001. Sensitivity analysis of crack detection in beams by wavelet technique. International Journal of Mechanical Sciences 43 (12), 2899–2910.
Ratcliffe, C.P., 1997. Damage detection using a modified Laplacian operator on mode shape data. Journal of Sound and Vibration 204 (3), 505–517.
Rucka, M., Wilde, K., 2006. Application of continuous wavelet transform in vibration based damage detection method for beams and plates. Journal of Sound and Vibration 297 (3–5), 536–550.
Salawu, O.S., 1997. Detection of structural damage through changes in frequency: a review. Engineering Structures 19 (9), 718–723.
Stubbs, N., Kim, J.T., 1996. Damage localization in structures without baseline modal parameters. AIAA Journal 34 (8), 1644–1649.
Wang, H., Qiao, P., 2008. On irregularity-based damage detection method for cracked beams. International Journal of Solids and Structures 45 (2), 688–704.
Yoon, M.K., Heider, D., Gillespie, J.W., et al., 2005. Local damage detection using the two-dimensional gapped smoothing method. Journal of Sound and Vibration 279 (1–2), 119–139.